One-dimensional overdriven detonations with branched-chain kinetics

Antonio L. Sánchez[a] and Manuel Carretero
Area de Mecánica de Fluidos, Departamento de Ingeniería Mecánica, Universidad Carlos III de Madrid, 28911 Leganés, Spain

Paul Clavin
Institut de Recherche sur les Phénomènes Hors Equilibre, Centre Universitaire de Saint-Jérôme, Service 252, 13397 Marseille, Cedex 20, France

Forman A. Williams
Center for Energy and Combustion Research, University of California San Diego, La Jolla, California 92093-0411

(Received 18 October 1999; accepted 5 December 2000)

The dynamics of time-dependent, planar propagation of gaseous detonations is addressed on the basis of a three-step chemistry model that describes branched-chain processes. Relevant nondimensional parameters are the ratio of the heat release to the thermal enthalpy at the Neumann state, the nondimensional activation energies for the initiation and branching steps, the ratio of the branching time to the initiation time and the ratio of the branching time to the recombination time. The limit of strong overdrive is considered, in which pressure remains constant downstream from the leading shock in the first approximation, and the ratio of specific heats γ is taken to be near unity. A two-term expansion in the strong overdrive factor is introduced, and an integral equation is derived describing the nonlinear dynamics and exhibiting a bifurcation parameter, the reciprocal of the product of $(\gamma-1)$, the nondimensional heat release and the nondimensional branching activation energy, with an acoustic correction. A stability analysis shows that, depending on values of the parameters, either the mode of lowest frequency or a mode of higher frequency may be most unstable. Numerical integrations exhibit different conditions under which oscillations die, low-frequency oscillations prevail, high-frequency oscillations prevail, highly nonlinear oscillations persist, or detonation failure occurs. This type of parametric analysis is feasible because of the relative simplicity of the model, which still is more realistic than a one-step, Arrhenius chemical approximation. In particular, by addressing the limit of slow radical recombination compared with branching, explicit results are derived for the critical value of the bifurcation parameter, involving the ratio of the recombination time to the induction time. The results help to clarify the general nature of one-dimensional detonation instability and provide simplifications that can be employed in efficiently relating gaseous detonation behavior to the true underlying chemistry. [DOI: 10.1063/1.1345880]

NOMENCLATURE

A	Frequency factor
b	Bifurcation parameter defined in (2.23)
b_c	Critical value of b at the Hopf bifurcation
b_{c_1}, b_{c_2}	Values of b_c for the two most unstable modes
$\overline{b}$	Modified bifurcation parameter defined in (5.19)
$\overline{b}_{c_1}, \overline{b}_{c_2}$	Critical values of $\overline{b}$ for the two most unstable modes
c_p	Specific heat at constant pressure
d	Overdrive parameter
E	Activation energy
F	Reactant
f	Normalized reactant mass fraction
k	Reaction-rate constant
$\mathbf{M}$	Third body
$[\mathbf{M}]$	Third-body concentration
P	Nondimensional period of the oscillations
Q	Amount of heat released per unit mass of radicals consumed
q	Nondimensional heat release
R	Universal gas constant
T	Temperature
T_c	Crossover temperature
t_i	Induction time, given in (2.15) for the hydrogen–oxygen system
u	Nondimensional gas velocity
v	Gas velocity relative to the shock of the steady detonation
W	Molecular weight
X	Radical
X_{O_2}	Oxygen mole fraction
x	Normalized radical mass fraction
Y_F	Initial reactant mass fraction
y	Geometrical coordinate
y_s	Location of the leading shock

[a]Electronic mail: asanchez@ing.uc3m.es

Greek Symbols

α Exponential growth rate of the temperature perturbation
β Nondimensional activation energy
γ Ratio of specific heats
Θ_N Reduced temperature increment at the Neumann spike $\beta_B \theta_N$
Θ_{N_c} Reduced crossover temperature defined in (3.2)
θ Nondimensional temperature increment
ε Ratio of the branching time to the recombination time evaluated at the Neumann spike of the steady detonation
$\overline{\varepsilon}$ Instantaneous value of the ratio of the branching time to the recombination time at the Neumann spike
κ Acoustic parameter defined in (4.1)
ν Ratio of the branching time to the initiation time evaluated at the Neumann spike of the steady detonation
$\overline{\nu}$ Instantaneous value of the ratio of the branching time to the initiation time evaluated at the Neumann spike
ξ Nondimensional mass-weighted coordinate defined in (2.2)
ξ_i Induction length defined in (2.14)
$\overline{\xi_i}$ Instantaneous value of the induction length defined in (5.9)
ρ Density
σ Complex exponential rate of the temperature perturbation
$\overline{\sigma}$ Acoustically modified exponential rate $(1+\kappa)\sigma$
τ Nondimensional time defined in (2.1)
ω Frequency of the temperature perturbation
$\overline{\omega}$ Modified frequency $(1+\kappa)\omega$

Subscripts

B Branching reaction
I Initiation reaction
N Properties at the Neumann spike
R Recombination reaction
∞ Properties far downstream from the leading shock

Superscripts

o Properties of the steady detonation

I. INTRODUCTION

Steady, planar detonation structure, first explained independently by Zeldovich, von Neumann, and Döring (ZND), involves a strong leading shock wave that heats the chemically reactive material and thereby causes exothermic chemical heat release to begin. The chemistry then proceeds in the high-speed subsonic flow behind the shock through chemical mechanisms that are gradually being understood better in recent years. The present paper addresses influences on detonation structure and dynamics of a model chemical mechanism that has been found to provide a very good description of the chemistry that occurs in most gaseous detonations. This description pertains to branched-chain chemical kinetics.[1]

The ZND detonation structure is now known to be unstable. Various instabilites in the inviscid flow associated with the chemical heat release generate disturbances that act back on the leading shock and cause the propagation to be unsteady and nonplanar. Much recent research has been devoted to trying to clarify further the nature of these instabilities (e.g., Refs. 2–4). In very strongly overdriven detonations, where the chemical heat release is sufficiently small compared with the thermal enthalpy behind the leading shock, ZND detonations in ideal gases must be stable because the corresponding shock wave is stable, but this situation is not usually encountered experimentally. Most real detonations are cellular, that is, they exhibit time-dependent, multidimensional structures that involve interactions of different shock waves under the influence of chemical heat release. There is interest in clarifying structures of cellular detonations. How the chemistry controls these structures is not well understood. It is known[4] that ZND detonations are multidimensionally unstable to any exothermic chemistry whatever, but the extent to which that instability affects the final cellular structure is unclear. While most investigators probably would agree that branched-chain kinetics of the type addressed here are significant in cellular detonation structure, the specific role of this chemistry has not been clarified.

As a first stage in improving understanding of the influence of this chemistry on cellular detonations, the present paper addresses the corresponding one-dimensional, time-dependent dynamics of unsteady, planar detonations. The planar problem is intrinsically simpler and yet sufficiently complex that much remains to be learned about it. In addition, one-dimensional, pulsating detonations, known as galloping detonations, have been observed experimentally. These generally occur for detonations under narrow confinement, where boundaries suppress the multidimensional, cellular behavior. The presence of the boundaries thus clearly influences galloping detonations. Since such boundaries are not present in the mathematical model addressed here, quantitative agreement of predictions with experiments on galloping detonations is not expected. Although there could be fortuitous agreement, the extent of agreement that should be anticipated currently is entirely unknown. The purpose of the present paper is not to develop a theory that is well justified for comparison with experiment on galloping detonations but rather to determine the influences of the branched-chain chemistry on the one-dimensional, time-dependent context. In this sense, the present work concerns a model problem designed to further advance our general understanding of the dynamics of gaseous detonations. In would be of interest in future work to study the extent to which the results can be compared with experiments on galloping detonations.

Most studies of planar detonation dynamics adopt one-

step chemistry approximations. Since chemistry affects detonation dynamics only by the sensible heat release that it produces through energy conservation, the only relevant difference between one-step and multistep chemistry is the number of first-order differential equations that need to be addressed to describe the chemical heat release. There are, for example, one-step approximations that can be anticipated to model branched-chain chemistry well,[1] and simpler models with similar attributes have been employed recently.[2–4] Most of the research exercising one-step chemistry, however, selects an exothermic Arrhenius process, usually of first order with respect to fuel, which does a poor job of capturing the separate initiation, branching and recombination steps of chain chemistry. There is, in addition, the possibility of more complex dynamics arising from the larger number of differential equations required for describing more complicated chemistry. For this reason, investigations of detonations with multistep model chemical kinetics are of interest.

The present paper addresses detonation dynamics with a model for branched-chain chemistry motivated by considerations of real chemistry, such as that of the hydrogen–oxygen system. The model is an extension of two-step chain-branching models often treated previously,[5–9] the extension being obtained by adding an initiation step to the branching and recombination steps. While the initiation step is unnecessary when chain carriers are initially present or in flames, where they arrive by diffusion, in detonations initiation is essential for the chemistry to begin. Although models including initiation are well known,[10–13] only two previous detonation studies appear to have addressed this type of kinetic scheme.[14,15] One[14] treated multidimensional stability, while the other[15] is the previous investigation that is most closely related to the present study, from the viewpoint of the problems addressed and the chemistry employed. The reader therefore is referred to Short and Quirk[15] for further background information.

The present study differs from that of Short and Quirk[15] in a number of ways. For example, the approximation is introduced here that the ratio of specific heats is near unity,[16] and the problem is formulated in terms of an integral equation that depends on the distribution of the heat-release rate, thereby extending an earlier development of this type[2] to include more detailed chemistry. These simplifications with respect to the previous work[15] lead to the occurrence of fewer nondimensional parameters whose values need to be specified in parametric investigations and permit more complete analytical developments, rather than necessitating fully numerical generation of results. Certain conclusions also differ. For example, it is found here that the most unstable mode is not always the one of lowest frequency; the analytical simplifications facilitate such discoveries. Analytical approximations are developed here that ultimately enable critical bifurcation values and frequencies to be obtained entirely in closed form with reasonable accuracy for realistic chemistry.

II. PROBLEM FORMULATION

A. Chemistry model

As in previous work,[15] we consider the initiation reaction

$$F \xrightarrow{\mathrm{I}} X,$$

the branching reaction

$$F + X \xrightarrow{\mathrm{B}} 2X$$

and the recombination reaction,

$$X \xrightarrow{\mathrm{R}} \text{Products},$$

where F and X represent the reactant and radical of the chemistry description. The reaction-rate constants of the first two reactions depend on the temperature, T, according to $k_I = A_I \exp[-E_I/(RT)]$ and $k_B = A_B \exp[-E_B/(RT)]$, where R is the universal gas constant, A_I and A_B are frequency factors and E_I and E_B are activation energies. The values of these two last quantities are such that the nondimensional activation energies $\beta_I = E_I/(RT_N^o)$ and $\beta_B = E_B/(RT_N^o)$ evaluated at the temperature of the steady detonation immediately downstream of the shock wave T_N^o are much larger than unity, thereby causing the rates of initiation and recombination to be very sensitive to small temperature variations. In typical chain-branching systems radical recombination involves three-body collisions with zero activation energy. The resulting temperature dependence of the associated rate constant is very weak and is, therefore, neglected in the present development, where we assume the rate constant of the recombination reaction, $k_R = A_R$, to be independent of temperature. Most of the heat is generated through radical recombination, with Q denoting here the amount of heat released per unit mass of radicals consumed in that step. The initiation step typically is endothermic and branching slightly exothermic, but their resulting enthalpy changes are of lesser importance and are considered here to be negligible. In the approximation employed, therefore, the energetics is the same as that considered previously.[15]

B. Conservation equations

To study the propagation of one-dimensional overdriven detonations with this chemistry, first let y denote the coordinate in a laboratory frame of reference, with $y_s(t)$ representing the instantaneous location of the leading shock wave. In order to parallel the simplified description given in Ref. 2, we consider the limit $(\gamma - 1) \ll 1$, with γ denoting here the ratio of specific heats. This assumption is reasonably well justified in fuel–air detonations, for which the elevated temperatures found downstream from the leading shock wave cause the specific heats to increase significantly, giving $\gamma \simeq 1.2$ in typical applications. In this limit of almost equal specific heats, the changes in temperature caused by pressure variations are negligible in the first approximation.[2] Also, in view of the large temperature sensitivity of the induction kinetics, which will be shown below to be mainly related to

the large value of β_B, only relatively small variations of the detonation propagation velocity from its steady value are considered. Furthermore, attention is restricted to overdriven detonations with large values of the overdrive parameter d, defined as the square of the ratio of the detonation propagation velocity to the velocity of the corresponding Chapman–Jouguet detonation.

As explained in previous publications,[2,3] the solution in this case (strongly overdriven detonations with almost equal specific heats and large temperature sensitivity of the induction kinetics) can be found by considering the distinguished limit $\beta_B \sim (\gamma-1)^{-1} \gtrsim d \gg 1$. At leading order, it is found that the spatial and temporal pressure variations downstream from the leading shock wave are negligible. Incorporating these simplifying assumptions reduces the leading-order problem to that of integrating the species and energy conservation equations, while mass conservation provides an integral constraint on the solution.[2] Acoustics enters in the solution as a first-order correction in the asymptotic development,[3] resulting in a modified integral constraint with corrections of order $d^{-1/2}$ to the critical conditions for the onset of instability and to the periods of the resulting oscillations. In what follows, we develop first the leading-order solution corresponding to the branched-chain kinetics considered here. The extension of the formulation to account for acoustic effects is presented later in Sec. IV.

To describe the solution, it is convenient to scale the time t with the constant recombination time A_R^{-1} according to

$$\tau = A_R t. \tag{2.1}$$

A dimensionless mass-weighted coordinate

$$\xi = \frac{A_R}{\rho_N^o v_N^o} \int_{y_s(t)}^{y} \rho(y',t)\, dy' \tag{2.2}$$

is then introduced, where ρ_N^o and v_N^o are the steady values at the Neumann spike (immediately behind the shock) of the density and gas velocity relative to the shock. The same notation will be employed throughout the following development: The superscript o will represent properties of the steady detonation, while the subscript N will denote the values of the flow variables at the Neumann spike.

For simplicity, an equal molecular weight, W, is assumed for all chemical species and a constant value of the specific heat at constant pressure, c_p, is employed. Changes in mean molecular weight and specific heat across the detonation can be expected to introduce relatively small quantitative corrections in the results, but the essential physics is captured with the simplifications introduced here, which allow the species and energy equations to be written as[4]

$$\frac{\partial x}{\partial \tau} + \frac{\partial x}{\partial \xi} = \frac{f}{\varepsilon}\{\nu \exp[\beta_I \theta/(1+\theta)] + \exp[\beta_B \theta/(1+\theta)]x\} - x, \tag{2.3}$$

$$\frac{\partial f}{\partial \tau} + \frac{\partial f}{\partial \xi} = -\frac{f}{\varepsilon}\{\nu \exp[\beta_I \theta/(1+\theta)] + \exp[\beta_B \theta/(1+\theta)]x\}, \tag{2.4}$$

$$\frac{\partial \theta}{\partial \tau} + \frac{\partial \theta}{\partial \xi} = qx, \tag{2.5}$$

while the continuity equation can be written in the form

$$\frac{\partial u}{\partial \xi} = \frac{\partial \theta}{\partial \tau} + \frac{\partial \theta}{\partial \xi}. \tag{2.6}$$

In the formulation, x and f denote, respectively, the mass fractions of the radical and the reactant scaled with the initial reactant mass fraction, Y_F. The variable $\theta = (T - T_N^o)/T_N^o$ measures temperature changes with respect to the temperature at the Neumann spike of the steady detonation, T_N^o. Mass conservation is expressed in terms of the scaled velocity $u = v/v_N^o$, where v is the gas velocity relative to the shock of the steady detonation. The heat of reaction Q per unit mass of fuel consumed is nondimensionalized to yield $q = (QY_F)/(c_p T_N^o)$, a parameter of order unity in overdriven detonations.[2] The particular chemistry addressed here enters the problem through four different parameters evaluated at $T = T_N^o$, namely, the two nondimensional activation energies $\beta_I = E_I/(RT_N^o)$ and $\beta_B = E_B/(RT_N^o)$, the ratio of the branching time to the recombination time $\varepsilon = A_R/[A_B \rho_N^o Y_F \times \exp(-\beta_B)/W]$ and the ratio of the branching time to the initiation time $\nu = [A_I \exp(-\beta_I)]/[A_B \rho_N^o Y_F \exp(-\beta_B)/W]$. In the branching step, the temperature dependence of the additional density factor has been included in β_B to avoid a clumsy and irrelevant factor of $(1+\theta)$ in the denominator.

Equations (2.3)–(2.6) must be integrated with appropriate initial and boundary conditions. In the stability study presented below, the initial profiles considered will be those of the steady detonation. On the other hand, at the Neumann spike ($\xi = 0$) the condition of inert flow across the shock wave yields $x = 0$ and $f = 1$, while the corresponding values of the temperature and velocity, $\theta = \theta_N(\tau)$ and $u = u_N(\tau)$, are functions of time related to the instantaneous propagation velocity of the leading shock through the Rankine–Hugoniot relationships. Since only small perturbations of the propagation velocity are considered, these relationships can be linearized to provide the equation

$$u_N = 1 - \frac{\theta_N}{\gamma - 1}. \tag{2.7}$$

To close the problem, a radiation condition must in general be imposed far downstream from the shock. In strongly overdriven detonations, in which the pressure perturbations are negligible, this radiation condition implies that the flow velocity must approach its steady value $u = u_\infty^o$ as $\xi \to \infty$.[2]

To find this value, and also the equilibrium temperature of the steady detonation, linear combinations of (2.3)–(2.6) can be integrated with $\partial/\partial\tau = 0$, and with $\theta_N^o = 0$ and $u_N^o = 1$, to give $\theta^o = q[1 - (x^o + f^o)]$ and $u^o = 1 + \theta^o$. As can be seen, when chemical equilibrium ($x^o = 0$ and $f^o = 0$) is approached far downstream, the nondimensional flow velocity and temperature of the steady detonation reach the values

$$u_\infty^o = 1 + q, \tag{2.8}$$

and $\theta_\infty^o = q$, respectively. This last result shows by integrating the steady form of (2.5) over the entire region downstream from the shock that the radical profile of the steady detonation satisfies

$$\int_0^\infty x^o d\xi = 1. \tag{2.9}$$

C. Chemical-kinetic parameters

Realistic values for the four chemical-kinetic parameters (β_B, β_I, ε, and ν) in general can be estimated for different chemical systems from their corresponding rate-limiting steps. For instance, in H_2-O_2 combustion, these rate-limiting steps are $H_2+O_2 \xrightarrow{1} 2OH$ (initiation), $H+O_2 \xrightarrow{2} OH+O$ (branching) and $H+O_2+M \xrightarrow{3} HO_2+M$ (recombination), where M represents a third body, its concentration being [M]. Values of the associated reaction-rate constants can be found in Ref. 17, for instance, yielding

$$\beta_I = 24131/T_N^o, \quad \beta_B = 8620/T_N^o, \tag{2.10}$$

$$\varepsilon = k_3[\mathrm{M}]/k_2 = 23.4p(T_N^o)^{-1.72}\exp(8620/T_N^o), \tag{2.11}$$

and

$$\nu = k_1/k_2 = 4.83\times 10^{-4}(T_N^o)^{0.7}\exp(-15511/T_N^o), \tag{2.12}$$

with the temperature T_N^o and post-shock pressure p expressed in K and bar, respectively.

The temperature dependence of the initiation and branching chemistry is seen from these values to be fairly strong, i.e., the conditions $\beta_I \gg 1$ and $\beta_B \gg 1$ are in general satisfied. It also can be seen that initiation reactions are very slow, so that the inequalities $\nu \ll 1$ and $\nu \ll \varepsilon$ always hold for temperatures of practical interest. As a result, the initial radical growth is very slow, and only negligibly small radical concentrations occur behind the shock throughout most of the so-called induction region. To estimate the length of this region, ξ_i, one can integrate the steady-state form of (2.3) with $f=1$ and $\theta=0$ to obtain the steady radical profile

$$x^o = \frac{\nu}{1-\varepsilon}[\exp[(1-\varepsilon)\xi/\varepsilon]-1], \tag{2.13}$$

which is approximately valid in the induction region. This equation reveals that radical mass fractions of order unity are reached only after an induction length

$$\xi_i = \frac{\varepsilon \ln(\nu^{-1})}{1-\varepsilon}, \tag{2.14}$$

which is a function of the two chemical-time ratios ε and ν. This nondimensional induction length can also be interpreted as the ratio of an induction time t_i to the recombination time A_R^{-1}. For the hydrogen–oxygen system, the predicted ignition time becomes

$$t_i = \frac{2.33\times 10^{-15}(T_N^o)^{1.7}\exp(8620/T_N^o)}{pX_{O_2}} \frac{\ln(\nu^{-1})}{1-\varepsilon}\,\mathrm{s}, \tag{2.15}$$

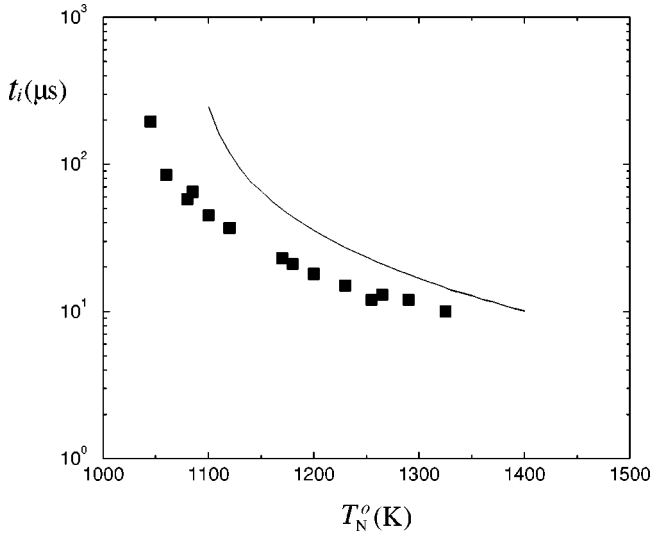

FIG. 1. The comparison of the induction time t_i measured in the shock-tube experiments of Bhaskaran *et al.* (Ref. 18) (squares) with the prediction of (2.15) with $p=2.5$ atm and $X_{O_2}=0.148$ (solid line).

where X_{O_2} represents the initial O_2 mole fraction and ε and ν can be evaluated from (2.11) and (2.12), respectively.

A great deal of shock-tube data exists on ignition times of hydrogen–oxygen systems. More than a dozen papers on this topic can be identified in the literature. Such experiments indeed are measurements on very highly overdriven steady, planar detonations in the present terminology, and therefore, it is possible to compare the predictions of (2.15) with these experimental results. As an example, we compare in Fig. 1 the induction times observed in the shock-tube experiments of Bhaskaran *et al.*[18] with those obtained from (2.15) for different values of T_N^o. In the experiments, the leading shock elevated the pressure of a stoichiometric mixture of hydrogen and oxygen diluted with 55.6% N_2 ($X_{O_2}=0.148$) to a fixed value $p=$ 2.5 atm. As can be seen, the agreement is reasonably good for the range of temperatures explored, with departures being somewhat more significant as the temperature decreases. Although Fig. 1 clearly indicates that the model chemistry used in this paper is relevant for hydrogen–oxygen systems, more careful comparisons with a larger number of experimental contributions would be necessary to evaluate the accuracy of (2.15) thoroughly. These comparisons are beyond the scope of the present work but are a suitable topic for future research.

For a given pressure the condition $\varepsilon=1$ determines the so-called crossover temperature, T_c (for example, $T_c \simeq 1500$ K at $p=40$ atm), that defines the second explosion limit of H_2-O_2 mixtures.[19] Equation (2.14) indicates that the induction length becomes infinite as the crossover temperature is approached. The chain-branching explosion is then replaced by a solution with small radical mass fractions, of order ν. Since $\nu \ll 1$, the time required to release an appreciable amount of heat in this regime of slow combustion becomes extremely large. Although the presence of the initiation step in the chemical model ensures that all of the heat is eventually released regardless of the initial temperature, for realistic values of ν the detonation thickness for T_N^o below crossover

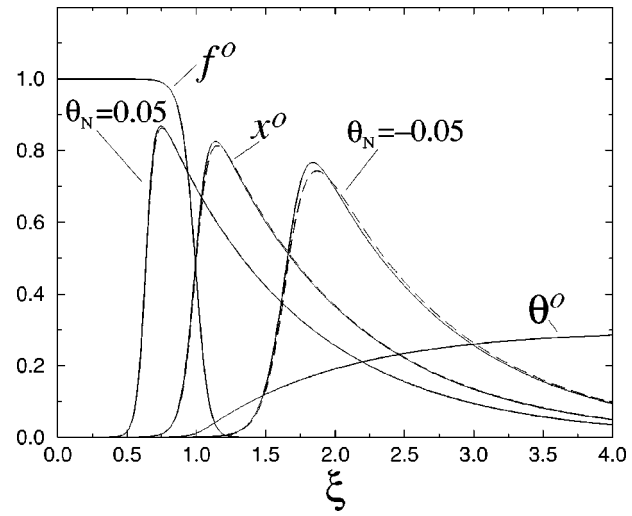

FIG. 2. The solid lines represent the steady profiles x^o, f^o and θ^o obtained by integration of (2.17)–(2.19) with $\varepsilon=0.05$, $\nu=5.60\times10^{-9}$, $\beta_B=10$, $\beta_I=10$ and $q=0.3$, and the corresponding modified radical profiles obtained for $\theta_N=\pm0.05$, while the dashed lines represent the approximate radical profiles obtained from Eq. (5.8).

is much too large to be significant. Therefore, in chain-branching systems of practical interest, e.g., hydrogen–oxygen mixtures, detonations can only develop for values of T_N^o above crossover, that is, values of ε smaller than unity. The ratio T_c/T_N^o was considered in previous work[15] to be a bifurcation parameter that was varied numerically to exhibit different types of solutions. Because of the exponential dependence of the branching rate on temperature, the value of ε becomes small as the Neumann temperature increases a small relative amount of order β_B^{-1} from crossover, so that small values of ε are found under most conditions, including in particular those of strong overdrives. In view of these considerations, we investigate in the following development the chemical-kinetic parameters in the ranges

$$\beta_B\sim\beta_I\gg1, \qquad \nu\ll\varepsilon\ll1, \tag{2.16}$$

as they apply to the description of overdriven detonations with chain-branching kinetics.

The detonation structure that arises in this limit is exhibited in Fig. 2, where the temperature and species profiles of the steadily propagating detonation, $\theta^o(\xi)$, $x^o(\xi)$, and $f^o(\xi)$, are plotted; dashed curves and those for $\theta_N\neq0$ in Fig. 2 are to be discussed later. These profiles are obtained by numerical integration of the equations

$$\frac{dx}{d\xi}=\frac{f}{\varepsilon}\{\nu\exp[\beta_I\theta/(1+\theta)]+\exp[\beta_B\theta/(1+\theta)]x\}-x, \tag{2.17}$$

$$\frac{df}{d\xi}=-\frac{f}{\varepsilon}\{\nu\exp[\beta_I\theta/(1+\theta)]+\exp[\beta_B\theta/(1+\theta)]x\}, \tag{2.18}$$

$$\frac{d\theta}{d\xi}=qx, \tag{2.19}$$

with $x=\theta=0$ and $f=1$ at $\xi=0$, the steady-state version of (2.3)–(2.5). The parametric values selected are $\varepsilon=0.05$, $\nu=5.60\times10^{-9}$, $\beta_B=10$, $\beta_I=10$ and $q=0.3$, with the chemical-time ratios chosen in this case such that $\xi_i=\varepsilon\ln\nu^{-1}/(1-\varepsilon)=1$. The induction, relatively rapid fuel consumption and slower radical recombination are evident in this figure.

D. Integral evolution equation

As explained in Ref. 2, the hyperbolic nature of (2.3)–(2.5) enables integration to be performed along the trajectories $\tau-\xi=$ constant. The composition and temperature of a given fluid particle thus can be obtained by solving (2.17)–(2.19) with initial conditions at $\xi=0$ given by $x=0$, $f=1$, and $\theta=\theta_N(\tau-\xi)$. The integration provides in particular the radical mass fraction of the fluid particle located at ξ at a given instant τ

$$x=x[\xi,\theta_N(\tau-\xi)], \tag{2.20}$$

as a function of the Neumann temperature $\theta_N(\tau-\xi)$ previously encountered by the fluid particle as it crossed the shock.

On the other hand, use of the expression for the heat-release rate appearing in (2.5), enables the integration of (2.6) to be performed to give

$$u_\infty^o-u_N=q\int_0^\infty x\,d\xi. \tag{2.21}$$

Combining now (2.7), (2.8), (2.20) and (2.21) finally gives the integral equation

$$\theta_N(\tau)=\frac{1}{\beta_B b}\left(\int_0^\infty x[\xi,\theta_N(\tau-\xi)]\,d\xi-1\right), \tag{2.22}$$

which controls the evolution of $\theta_N(\tau)$, thereby determining the dynamical behavior of the detonation. Following the analysis of Clavin and He,[2] the bifurcation parameter

$$b=\frac{1}{(\gamma-1)\beta_B q}, \tag{2.23}$$

has been introduced in writing (2.22). Because the heat release occurs through recombination, the radical profile enters in the problem as an appropriately normalized heat-release distribution. In view of (2.9), it is clear that steady detonations, those having $\theta_N(\tau)=0$ and $x(\xi,0)=x^o(\xi)$, arise as one of the possible solutions to (2.22). It is shown below that such steady solutions are stable only for values of the bifurcation parameter b above a critical value, at which the solution undergoes a Hopf bifurcation. The b of (2.23) is evidently different from T_c/T_N^o, the crossover temperature ratio previously[15] termed a bifurcation parameter, but it bears some relationship to it, as will be seen. Equation (2.22) also indicates that in the absence of chemical reaction the normalized constant temperature associated with the remaining piston-supported shock wave is

$$\theta_N=-\frac{1}{\beta_B b}. \tag{2.24}$$

This value is clearly associated in particular with the solution that arises when detonation quenching takes place.

Figure 2 shows effects of the variations of the leading shock on the shape of the heat-release distribution $x[\xi,\theta_N]$ that appears in the integral equation. In particular, radical profiles corresponding to $\theta_N=\pm 0.05$ are plotted along with the steady distribution $x^o(\xi)=x[\xi,\theta_N=0]$. As anticipated in the development leading to (2.22), small variations of the shock propagation velocity, i.e., values of $\theta_N \ll 1$, are amplified through the chemistry to give much larger changes in the heat-release distribution. For the particular values of θ_N used in the plot, the profile $x[\xi,\theta_N=0]$ undergoes both a translation of order unity and a non-negligible change of shape. It is shown below that this large temperature sensitivity is mainly associated with the large activation energy of the branching step, β_B.

III. STABILITY AND NONLINEAR DYNAMICS OF THE SOLUTION

There are numerous physical situations in which stable solutions become unstable when a parameter passes through a critical value, beyond which time-dependent behavior occurs. The laminar boundary layer is a classical example that exhibits instability above a critical Reynolds number. A corresponding bifurcation parameter for the present detonations is the temperature-sensitivity parameter b^{-1}. Investigations of departures from stable behavior can be made by solving the governing equations numerically for different values of b with different initial conditions. Stabilities of steady solutions also can be investigated analytically by introducing small perturbations. Both of these approaches are pursued here to ascertain how the behavior of the system varies with b. Appropriate mathematical methods vary, involving algebraic equations, differential equations or integral equations, depending on the problem. Integral equations are involved in the present problem.

To investigate the behavior of the solution as the bifurcation parameter b is decreased, numerical integrations of the nonlinear evolution equation (2.22) were carried out. In the computations, the values $\beta_B=\beta_I=10$ and $q=0.3$ were selected for the nondimensional activation energies and heat of reaction, respectively. Results including two different branching times, $\varepsilon=0.15$ and $\varepsilon=0.05$, were computed, with the associated values for the initiation time $\nu=3.46\times10^{-3}$ and $\nu=5.60\times10^{-9}$ selected to give the nondimensional induction length $\xi_i=1$, that is, the induction time t_i equal to the recombination time. Variations of ε and ν about these values also were investigated. Integration along the characteristics (2.17)–(2.19) was performed with a fourth-order Runge–Kutta scheme with adaptive step size, and a Newton–Cotes method was employed for the quadrature appearing in (2.22). To facilitate the potential development of instabilities, an initial perturbation intentionally was introduced externally by employing a low-accuracy scheme (second-order Runge–Kutta) in the computation of the starting steady profiles. For each calculation, the extension of the computational domain was varied to accommodate the maximum induction length observed, with a maximum induction length equal to 100 used near quenching. A uniformly distributed grid of up to 32 000 points was used to discretize the flow field. This uniform grid was distributed along the positive τ and ξ axes, while the adaptive Runge–Kutta scheme marched along the characteristics in integrating (2.17)–(2.19).

A. The Hopf bifurcation

The computations revealed that for values of the bifurcation parameter b above a critical value b_C the steady detonation remains stable, i.e., the steady solution $\theta_N=0$ is eventually recovered after a transition stage in which the initial perturbation exponentially decays to zero. On the other hand, as b is decreased below b_C the initial perturbation is seen to grow, leading to an oscillatory solution of finite amplitude. To characterize the solution at the onset of the instability, a linear stability analysis of the steady solution was performed. Introducing into (2.22) infinitesimally small values of the temperature perturbation, θ_N, with an exponential time dependence of the form $\theta_N \propto \exp(\sigma\tau)$ leads to

$$b=\int_0^\infty \frac{1}{\beta_B}\left(\frac{dx}{d\theta_N}\right)_{\theta_N=0} \exp(-\sigma\xi)\,d\xi, \tag{3.1}$$

as an implicit equation for $\sigma=\alpha+\omega i$. To compute the above integral, system (2.17)–(2.19) was differentiated with respect to θ_N, providing three new ordinary differential equations for the functions $dx/d\theta_N$, $df/d\theta_N$, and $d\theta/d\theta_N$. Integrating then the resulting system of six differential equations with initial conditions $x=f-1=\theta=dx/d\theta_N=df/d\theta_N=d\theta/d\theta_N-1=0$, as corresponds to $\theta_N=0$, provides in particular the function $(dx/d\theta_N)_{\theta_N=0}$ required to solve (3.1). A two-dimensional Newton iteration in the complex number σ was then performed to identify the values for which solutions exist; the convergence criterion adopted typically was one part in 10^{-4}, and no convergence difficulties were encountered. Equation (3.1) applies only for unstable, neutral and relatively weakly stable modes because the integral diverges for $\alpha<-1$, an uninteresting range that was not investigated.

The growth rate α and the frequency ω corresponding to the two modes with larger growth rate are shown in Fig. 3 for the sets of chemical-kinetic parameters studied here, and for decreasing values of the bifurcation parameter b. As previously anticipated, a Hopf bifurcation takes place as b is decreased below a critical value. The frequency values, and the corresponding values of b of the neutrally stable solution of the modes with the two lowest frequencies are given in Table I. In Fig. 3 a different mode is seen to be associated with the instability of the steady solution for the two different sets of conditions. Thus, for conditions sufficiently far above crossover, as it is the case $\varepsilon=0.05$, the mode of higher frequency dominates as the steady solution becomes unstable, while for larger values of the reduced branching time ε the Hopf bifurcation occurs first at the lower frequency. In comparison, for the particular conditions addressed by Short and Quirk,[15] the Hopf bifurcation encountered was of the low-frequency type, with the other mode

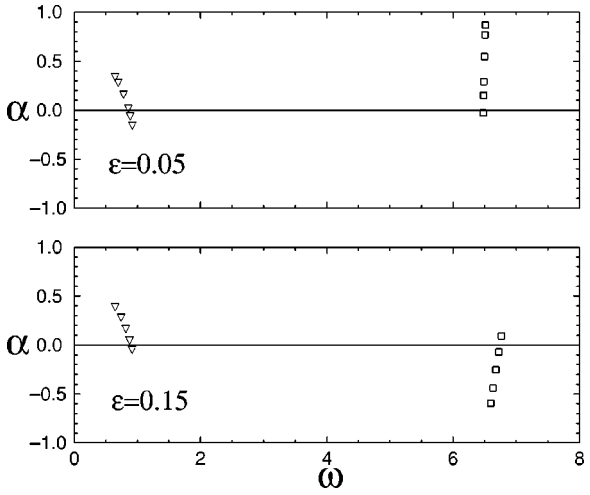

FIG. 3. The values of α and ω of the two modes of smaller frequency for $\xi_i=1.0$, $\beta_B=\beta_I=10$ and $q=0.3$ as obtained from (3.1) with $\varepsilon=0.05$ ($b=0.90,0.75,0.65,0.50,0.40,0.36$) and with $\varepsilon=0.15$ ($b=0.65,0.55,0.45,0.37,0.31$).

only appearing marginally as a decaying perturbation of the different solutions computed.

B. The development of the oscillatory instability

The time evolution of the solutions corresponding to $\varepsilon=0.15$ and $\varepsilon=0.05$ is exhibited in Figs. 4 and 5, respectively. To allow comparisons with subsequent analytical results, the reduced variable $\Theta_N=\beta_B\theta_N$ is employed in the plots, a selection that (3.1) indicates is appropriate. The discussion here addresses only the upper curves in these figures, the lower curves being considered in the following subsection.

As can be seen from Fig. 4, the growth rate of the second mode in the case $\varepsilon=0.15$ is sufficiently negative for its effect to be always negligible for all the cases shown. For $b<b_{C_1}=0.593$ the initial perturbation grows in time to give a long-period oscillatory solution, as can be observed for instance in the case $b=0.55$. Qualitatively similar results are obtained as b is initially decreased from b_{C_1}, with the resulting oscillations showing increasing amplitudes. The associated periods increase from the value $P=2\pi/\omega=7.00$ predicted by the linear stability analysis at $b=b_{C_1}$. The linear stability analysis is not able to predict the increase in period away from the bifurcation point accurately. For instance, for $b=0.55$ and $b=0.45$ the corresponding periods of oscillations are $P=7.34$ and $P=9.38$, while the linear stability analysis yields $P=7.15$ and $P=7.67$. In the solution that emerges, the Neumann temperature, which is directly related to the propagation velocity of the leading shock wave, is seen to remain below that of the steady solution most of the time, exhibiting large overshoots of relatively short length. Qualitatively similar oscillations are found in previous numerical studies.[2,15]

In the case $\varepsilon=0.05$ exhibited in Fig. 5, both of the

TABLE I. The critical values of b (and the corresponding frequencies) of the neutrally stable solution of the modes with the two lowest frequencies as obtained from Eq. (3.1).

	$\varepsilon=0.05$	$\varepsilon=0.10$	$\varepsilon=0.15$
$\nu=5.60\times10^{-9}$:			
b_{C1} (ω_{C1})	0.667 (0.864)	1.031 (0.523)	1.276 (0.374)
b_{C2} (ω_{C2})	0.873 (6.478)	1.855 (3.183)	2.904 (2.075)
$\nu=1.23\times10^{-4}$:			
b_{C1} (ω_{C1})	0.374 (1.346)	0.646 (0.877)	0.861 (0.660)
b_{C2} (ω_{C2})	0.268 (13.36)	0.593 (6.579)	0.969 (4.308)
$\nu=3.46\times10^{-3}$:			
b_{C1} (ω_{C1})	0.245 (1.719)	0.435 (1.155)	0.593 (0.897)
b_{C2} (ω_{C2})	0.090 (20.64)	0.205 (10.22)	0.343 (6.735)

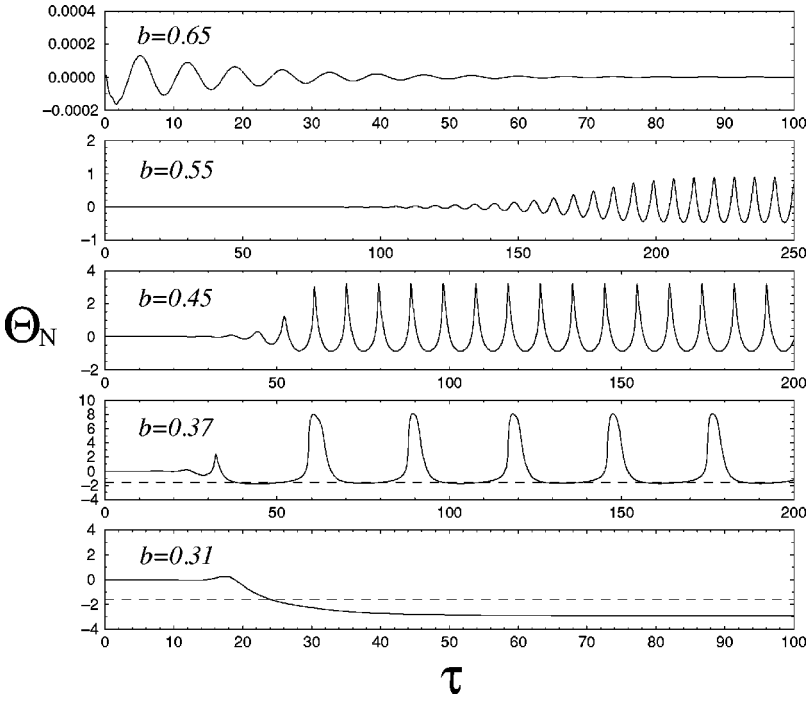

FIG. 4. The time evolution of $\Theta_N=\beta_B\theta_N$ for decreasing values of the bifurcation parameter b as obtained from (2.22) with $\varepsilon=0.15$, $\nu=3.46\times10^{-3}$, $\beta_B=10$, $\beta_I=10$, and $q=0.3$.

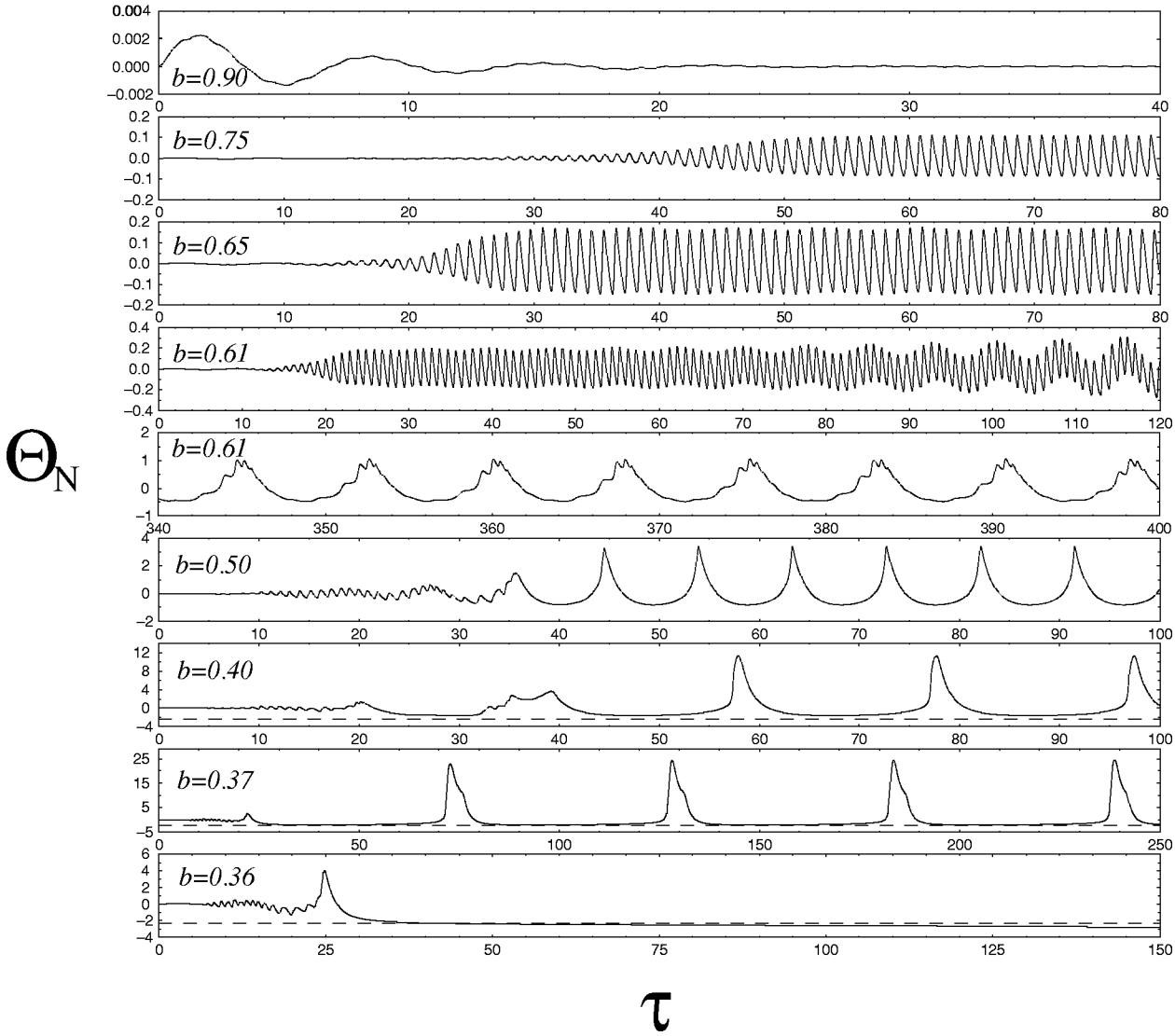

FIG. 5. The time evolution of $\Theta_N=\beta_B\theta_N$ for decreasing values of the bifurcation parameter b as obtained from (2.22) with $\varepsilon=0.05$, $\nu=5.60\times10^{-9}$, $\beta_B=10$, $\beta_I=10$ and $q=0.3$.

modes identified above can be observed in the decaying transient solution corresponding to $b>b_{C_2}=0.873$. For b in the range $0.873>b>0.667$ the linear stability analysis predicts that the first mode remains stable, while the second mode does not. This is illustrated for $b=0.75$, a case for which the long-period oscillation associated with the first mode is seen to decay, while the second mode grows exponentially to finally give an oscillatory solution of period $P=0.97$. Similar results are obtained as $b>b_{C_1}$ is further decreased from b_{C_2}; the resulting oscillations have increasing amplitudes, whereas the period remains practically invariant, and in agreement with the results of the linear stability analysis. Note that the shape of the oscillations is markedly different from that of the oscillations associated with the long-period mode seen in Fig. 4.

As expected from the results of the linear stability analysis, the rate of decay of the long-period oscillations decreases as b is decreased, so that their effect remains in the solution for a longer time. The results corresponding to $b=0.65$ indicate that this long-period modulation decays away even for values of b below $b_{C_1}=0.667$. The resulting behavior changes as b reaches a value $b\simeq0.64$, for which the amplitude of the long-period oscillations is seen to increase with time. The resulting time evolution is seen in the two plots corresponding to $b=0.61$. Although the oscillations corresponding to the second mode appear earlier because of their associated larger growth rate, the long-period oscillations also develop, so that both modes are eventually present in the resulting solution for long times. This behavior is seen in all solutions for b in the range $0.64>b>0.59$. As the bifurcation parameter is further decreased to $b=0.58$, the effect of the second mode is restricted to the initial transient, and a long-period oscillatory solution arises for large times, as seen in Fig. 5 for $b=0.50$. The period of the emerging solution, $P=9.40$, differs from the value $P=8.01$ associated with the first mode in the linear stability analysis for $b=0.50$. When the value of b is further decreased, the transition to the long-period oscillatory mode is faster and results in oscillations with increased values of both the amplitude and the period, in agreement with the behavior shown in Fig. 4.

C. The crossover temperature: Dynamic quenching

Failure of the detonation is observed as the minimum temperature of the oscillatory solution approaches the crossover value, a behavior previously encountered in Ref. 15. The branching time associated with each fluid particle depends on the temperature increase that it experiences as it crosses the shock wave. As can be concluded from (2.17),

$$\Theta_{N_c}=\beta_B\left(\frac{T_c}{T_N^o}-1\right)=\frac{\ln(\varepsilon)}{1-\ln(\varepsilon)/\beta_B}, \tag{3.2}$$

defines the reduced crossover temperature at which the initial rates of branching and recombination are equal. Evaluating the above expression for $\beta_B=10$ gives $\Theta_{N_c}=-2.305$ and $\Theta_{N_c}=-1.595$ for $\varepsilon=0.05$ and $\varepsilon=0.15$, respectively. Fluid particles with $\Theta_N<\Theta_{N_c}$ release only a small amount of heat, of order ν, as they cross the detonation. This reduced energy input leads to smaller propagation velocities and to even larger branching times, thereby eventually causing the failure of the detonation.

This mechanism of detonation failure is illustrated in Fig. 5, where dashed lines represent the crossover temperature corresponding to $\varepsilon=0.05$. As the minimum postshock temperature approaches the crossover value, the period of the associated detonation increases. For instance, the solution for $b=0.37$ has a period $P=55.24$ with a minimum temperature $\Theta_N=-2.08$. Transition from the steady detonation with $\Theta_N=0$ to the chemically frozen shock wave takes place when the minimum temperature falls below crossover during the initial transient regime, a phenomenon clearly observed for $b=0.36$. In the small intermediate parametric range $0.37>b>0.36$ the solution becomes very dependent on the accuracy of the numerical scheme and on the length of the integration domain. Although transition to chaos may occur in this parametric range (as observed away from the bifurcation point in previous numerical studies[2,15]), this question is not investigated further here because the range is small and the adopted integration techniques inappropriate. It may be noted that, in the quasi-frozen solution that emerges at the smallest value of b shown, the radical mass fraction is of order ν, yielding $\Theta_N\simeq-1/b$ for the post-shock temperature, a result previously anticipated in (2.24). Clearly, quenching of a piston-supported detonation may take place only when the temperature increase of the associated nearly chemically frozen shock wave is such that $-1/b<\Theta_{N_c}$.

A similar behavior is seen in Fig. 4. Because of the relatively large value of ν employed in this case, nonnegligible heat release can also take place for Θ_N slightly below Θ_{Nc}. Pulsating oscillations with minimum Neumann temperatures below crossover, therefore, can exist, as seen for $b=0.37$. When the bifurcation parameter is reduced to $b=0.31$, this regime is no longer observed, and detonation quenching appears.

IV. ACOUSTIC EFFECTS IN MODERATELY OVERDRIVEN DETONATIONS

The results presented above assume constant pressure, as corresponds strictly to infinitely large values of d, thereby neglecting the small pressure variations that appear in overdriven detonations with finite overdrives. These acoustic effects can be incorporated by introducing asymptotic expansions for the flow variables in powers of the small parameter

$$\kappa=\left(\frac{\gamma+1}{8\gamma}\,\frac{q+1}{q}\,\frac{1}{d}\right)^{1/2}, \tag{4.1}$$

of order $d^{-1/2}$, a development presented elsewhere.[3] The first-order correction is found to enter in the solution by modifying the leading-order integral constraint (2.22) to give

$$\theta_N(\tau)=\frac{1}{\beta_B b(1+\kappa)}\times\left(\int_0^\infty x\{\xi,\theta_N[\tau-(1+\kappa)\xi]\}d\xi-1\right). \tag{4.2}$$

Consideration of infinitesimally small temperature perturbations, θ_N, then leads to

$$b(1+\kappa)=\int_0^\infty\frac{1}{\beta_B}\left(\frac{dx}{d\theta_N}\right)_{\theta_N=0}\exp(-\sigma(1+\kappa)\xi)d\xi, \tag{4.3}$$

as a replacement for (3.1). Comparison of (4.2) and (4.3) with their acoustic-free versions (2.22) and (3.1) suggests that, for overdriven detonations with d sufficiently larger than unity, the effect of acoustics is limited to small corrections, of order $\kappa\sim d^{-1/2}$, to the period and amplitude of the oscillations and to the critical value of the bifurcation parameter b. The acoustic effects do not introduce qualitative modifications for overdriven waves. Since in most applications the overdrive factor d remains below $d\simeq5$, these acoustic corrections must however in general be considered for increased accuracy.

Since the perturbative analysis leading to (4.2) and (4.3) uses d as an asymptotically large quantity, the resulting equations do not apply when d is of order unity, that is, for weakly overdriven or Chapman–Jouguet detonations. Nevertheless, since the development used here embodies the key physics underlying the planar detonation instability, no new phenomena are expected to arise as the degree of overdrive is decreased, with differences in the stability character of the resulting detonations being only quantitative. This can be illustrated by direct comparison of the results of the present analysis with those obtained by Short and Quirk[15] for a near-Chapman–Jouguet detonation with $d=1.2$. Their numerical work employs the crossover temperature T_c/T_N^o as a bifurcation parameter, with the rate of the initiation reaction at the Neumann spike $\nu/\varepsilon=1.62\times10^{-6}$ and the remaining parameters $q=3$, $\beta_B=8$, $\beta_I=20$, and $\gamma=1.2$ being held constant in the computations. Evaluating (4.1) with these parametric values yields $\kappa=0.505$ for the acoustic parameter, no longer a small quantity as a result of the weak overdrive.

The evolution with T_c/T_N^o of the growth rate and of the frequency of the two most unstable modes obtained from a normal mode linear stability analysis of the complete numerical solution (Fig. 2 in Ref. 15) are compared in Fig. 6 with the solution of (4.3). The value of $\varepsilon=\exp[\beta_B(1-T_N^o/T_c)]$ can be extracted from (3.2) as a function of the

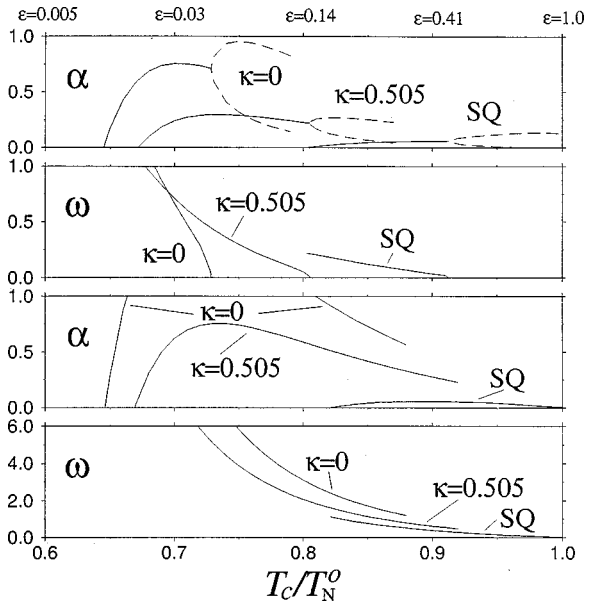

FIG. 6. The values of α and ω of the two modes of smaller frequency for $q=3$, $\beta_B=8$, $\beta_I=20$, and $\gamma=1.2$ as obtained from the stability analysis of the complete numerical problem with $F=1.2$ (SQ), from (4.3) with $\kappa=0$ and from (4.3) with $\kappa=0.505$ (purely real roots are represented with dashed lines).

crossover temperature. Therefore, the parametric study in Ref. 15 for increasing values of T_c/T_N^o with $\beta_B=8$ corresponds in the present formulation to a parametric study in the branching rate ε, with $\nu=1.62\times10^{-6}\varepsilon$ and with the parameter $b=[(\gamma-1)\beta_B q]^{-1}=0.208$ being held constant. Results corresponding to the isobaric model ($\kappa=0$) are exhibited in the plot along with those obtained with $\kappa=0.505$.

As can be seen, our analysis correctly predicts the qualitative behavior of both stability modes. For instance, (4.3) reproduces the pitchfork bifurcation associated with the mode of lower frequency, as well as the qualitative variation of α and ω for the higher-frequency mode. However, as previously anticipated, the quantitative agreement is poor, with the results of our analysis overestimating significantly the frequencies and the growth rates of both modes. Also, (4.3) fails to give the critical crossover temperature at the onset of instability; the exact solution tends to be more stable than the predictions derived with strong overdrives. It is however remarkable how the first-order correction for the acoustics improves significantly the quantitative results of the isobaric approximation, further supporting the use of (4.3) for calculating the stability characteristics of moderately overdriven detonations.

V. THE LIMIT OF SLOW RADICAL RECOMBINATION

The limit $\varepsilon\ll1$, with post-shock temperatures far above the crossover value, is amenable to development of an analytic description of the solution and reflects realistic conditions for many detonations. The analysis of this limit to be derived here will provide, in particular, a simplified explicit expression for the evolution equation (4.2) that reproduces the nonlinear dynamics previously exhibited in Figs. 4 and 5 with reasonable accuracy. This limit also serves to identify the key parameters that control the stability of the detonation and to determine, through a linear stability analysis of the resulting simplified description, the parametric dependence of each of the modes of instability that were previously discussed.

A. Asymptotic description for the heat-release law

Guided by the previous estimates, we select the initiation rate such that $\nu\ll\varepsilon$ and consider, in particular, the distinguished limit $\varepsilon\ln\nu^{-1}\sim1$, for which the induction length ξ_i of (2.14) is of order unity. Three different regions can then be observed in the internal structure exhibited in Fig. 2. There exists an induction region that extends over $0<\xi<\xi_i$ in which x is exponentially small, with the effect of initiation being relevant only in a sublayer of thickness ε in this layer, located immediately downstream from the shock wave, where x is of order ν. The effect of branching then causes x to grow slowly, eventually increasing to values of order unity at $\xi\simeq\xi_i$. There then exists a thin branching layer of thickness $\varepsilon\ln(\varepsilon^{-1})$ across which fuel consumption is important. After fuel is depleted, radical recombination is the only chemical process that remains active, giving an exponentially decreasing x profile, as can be anticipated from (2.17) with $f=0$. This general type of behavior has been seen in earlier work.[20–22]

With $\varepsilon\ll1$ the effect of radical recombination is very limited in both the induction region and the branching layer. When heat release is associated only with radical recombination, the temperature remains approximately constant until after the initiation and branching reactions are frozen, and it is therefore justified to neglect the spatial variation of k_I and k_B to study the evolution of the system. To see this more precisely, note that the temperature increment in the initial layer where initiation is significant can be estimated from (2.19) to be of order $q\varepsilon\nu$. Therefore, the temperature variation of the initiation reaction can be neglected altogether in (2.17)–(2.18) as long as the criterion $q\varepsilon\nu\beta_I\ll1$ is satisfied. Similarly, since the thickness of the branching region, where x is of order unity, is of order $\varepsilon\ln(\varepsilon^{-1})$, the temperature increase that occurs prior to fuel depletion is a small quantity of order $q\varepsilon\ln(\varepsilon^{-1})$, and can safely be neglected as long as $q\varepsilon\ln(\varepsilon^{-1})\beta_B\ll1$. Even with non-neutral energetics of initiation and branching, in view of the small extent to which initiation proceeds, enthalpy changes associated with these two steps remain negligible, provided only that the heat release in chain branching is small compared with that in recombination.

If these conditions are satisfied, then θ can be replaced by θ_N in (2.17) and (2.18) to yield the problem

$$\frac{dx}{d\xi}=\frac{f}{\varepsilon}\{\overline{\nu}+x\}-x, \tag{5.1}$$

$$\frac{df}{d\xi}=-\frac{f}{\varepsilon}\{\overline{\nu}+x\}, \tag{5.2}$$

$$x(0)=0,\quad f(0)=1, \tag{5.3}$$

where

$$\overline{\varepsilon}=\exp\left[-\frac{\beta_B\theta_N}{1+\theta_N}\right]\varepsilon,$$
$$\overline{\nu}=\exp[(\beta_I-\beta_B)\theta_N/(1+\theta_N)]\nu, \tag{5.4}$$

are the modified values of the chemical-time ratios associated with the instantaneous post-shock temperature. Note that if departures from the steady solution are limited to values of θ_N such that $\beta_B\theta_N$ and $(\beta_I-\beta_B)\theta_N$ remain no larger than order unity, then the limit $\nu\ll\varepsilon\ll 1$ with $\varepsilon\ln\nu^{-1}\sim 1$ also implies that

$$\overline{\nu}\ll\overline{\varepsilon}\ll 1 \quad \text{and} \quad \overline{\varepsilon}\ln\overline{\nu}^{-1}\sim 1, \tag{5.5}$$

yielding the same type of limit for these functions.

The solution to (5.1)–(5.3) in the distinguished limit (5.5) can be computed by matched asymptotic expansions. The development, which is not included here, is a straightforward extension of previous work on a related chain-branching–chain-breaking problem.[23] The asymptotic analysis provides in particular the reduced representation

$$x=\frac{\overline{\nu}\{\exp[(1-\overline{\varepsilon})\xi/\overline{\varepsilon}]-1\}}{1+\overline{\nu}\exp[(1-\overline{\varepsilon})\xi/\overline{\varepsilon}]}\times(1-\overline{\varepsilon}\ln\{1+\overline{\nu}\exp[(1-\overline{\varepsilon})\xi/\overline{\varepsilon}]\}), \tag{5.6}$$

for the radical profile, an expression valid in the first approximation until fuel is depleted at $\xi=\overline{\varepsilon}\ln(\overline{\nu}^{-1}\overline{\varepsilon}^{-1})/(1-\overline{\varepsilon})$. This expression must be supplemented by the approximate profile

$$x=(1-\overline{\varepsilon}\ln\overline{\varepsilon}^{-1})\exp\left[-\left(\xi-\frac{\overline{\varepsilon}\ln(\overline{\nu}^{-1}\overline{\varepsilon}^{-1})}{1-\overline{\varepsilon}}\right)\right], \tag{5.7}$$

corresponding to the recombination region. Combining now (5.6) and (5.7) finally gives the approximate expression

$$x[\xi,\theta_N]=\frac{1+H(\xi-\overline{\xi}_i)\{\exp[-(\xi-\overline{\xi}_i)]-1\}}{1+\exp[-(1-\overline{\varepsilon})(\xi-\overline{\xi}_i)/\overline{\varepsilon}]}, \tag{5.8}$$

where $H()$ denotes the Heaviside step function. The dependence on θ_N enters in (5.8) through $\overline{\varepsilon}$ and also through the modified induction length

$$\overline{\xi}_i=\frac{\overline{\varepsilon}\ln\overline{\nu}^{-1}}{1-\overline{\varepsilon}}, \tag{5.9}$$

at which the radical profile given in (5.8) reaches a value $x=1/2$. The accuracy of the above representation is tested in Fig. 2, where the radical profiles obtained from (5.8) for $\theta_N=(0,\pm 0.05)$ are compared with numerical integrations of the original problems (2.17)–(2.19). As can be seen, the asymptotic description describes with excellent accuracy the shape of the heat-release distribution and its changes with the Neumann temperature.

B. The simplified evolution equation

In writing the integral evolution equation (4.2) associated with the simplified description (5.8) it is important to realize that the main dependence of x on θ_N is due to the

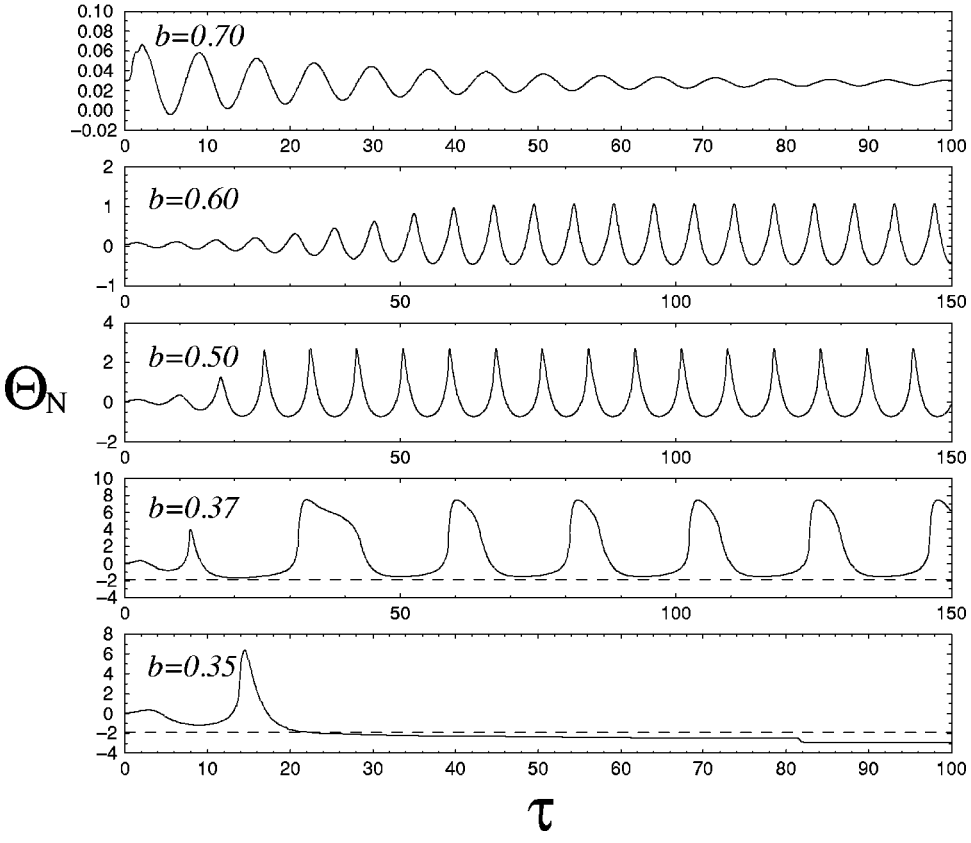

FIG. 7. The time evolution of $\Theta_N=\beta_B\theta_N$ for decreasing values of the bifurcation parameter b as obtained from (5.10) with $\kappa=0$, $\varepsilon=0.15$ and $\nu=3.46\times10^{-3}$.

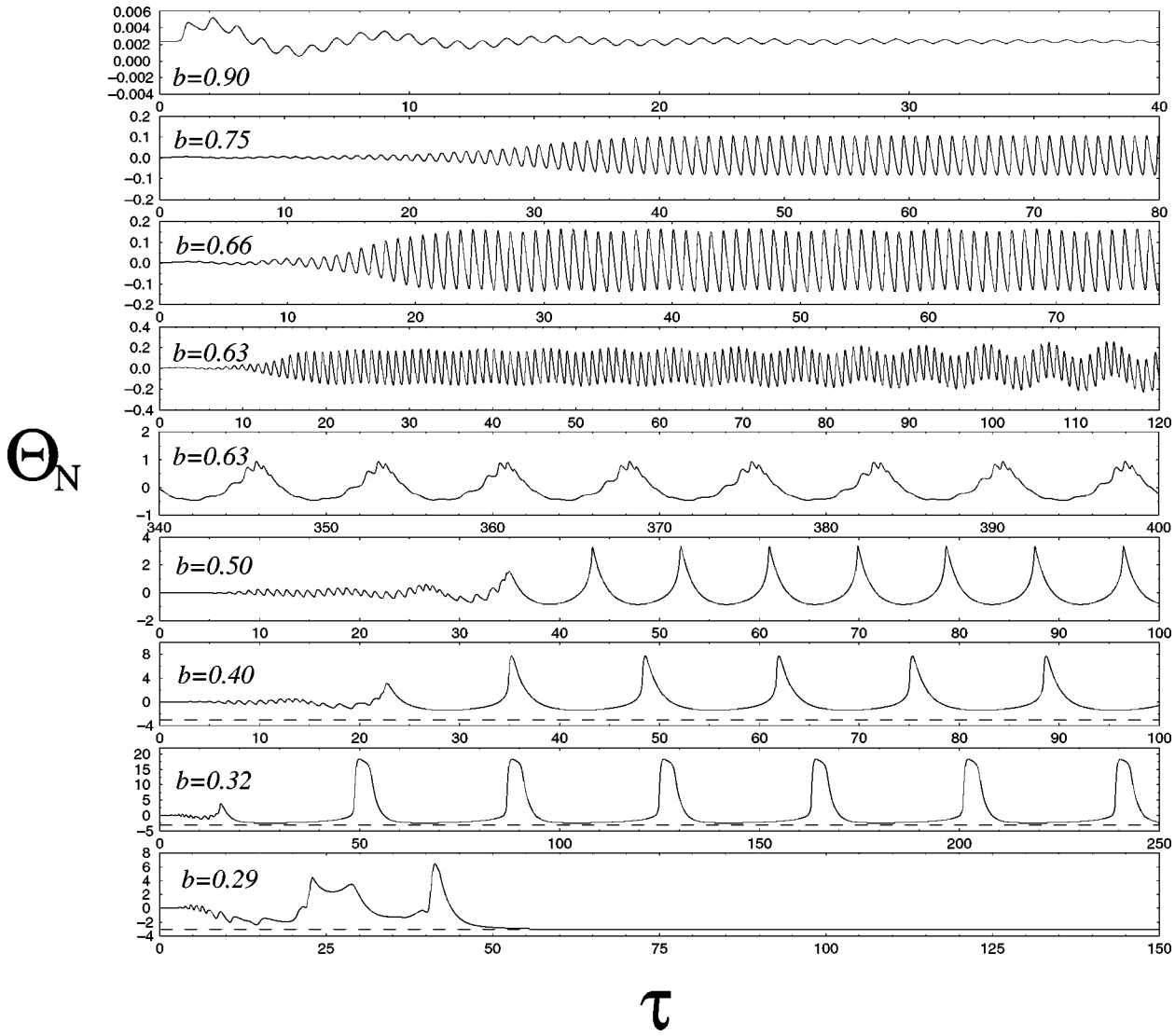

FIG. 8. The time evolution of $\Theta_N=\beta_B\theta_N$ for decreasing values of the bifurcation parameter b as obtained from (5.10) with $\kappa=0$, $\varepsilon=0.05$ and $\nu=5.60\times10^{-9}$.

exponential variation of the branching time $\overline{\varepsilon}$, while the variation of $\ln\overline{\nu}^{-1}$ from its steady value $\ln\nu^{-1}$ can be neglected in the first approximation. Furthermore, small values of θ_N of order β_B^{-1} yield changes of x of order unity, so that it is appropriate to define a rescaled variable of order unity $\Theta_N=\beta_B\theta_N$. Introducing then (5.8) into (4.2) produces the evolution equation

$$b\Theta_N(\tau)=\int_0^\infty \frac{1+H(\xi-\overline{\xi}_i)\{\exp[-(\xi-\overline{\xi}_i)]-1\}}{1+\exp[-(1-\overline{\varepsilon})(\xi-\overline{\xi}_i)/\overline{\varepsilon}]}d\xi-1. \tag{5.10}$$

In the present approximation, the time-dependent functions $\overline{\varepsilon}[\tau-(1+\kappa)\xi]$ and $\overline{\xi}_i[\tau-(1+\kappa)\xi]$ can be written from (5.4) and (5.9) as

$$\overline{\varepsilon}=\varepsilon\exp\{-\Theta_N[\tau-(1+\kappa)\xi]\},$$
$$\overline{\xi}_i=\frac{\varepsilon\ln\nu^{-1}}{\exp\{-\Theta_N[\tau-(1+\kappa)\xi]\}-\varepsilon}, \tag{5.11}$$

where a Frank–Kamenetskii linearization has been adopted for the exponential temperature dependence of the branching reaction rate. The definition of $\overline{\varepsilon}$ given in (5.11) yields in the present approximation $\Theta_{N_c}=\ln(\varepsilon)$ for the crossover temperature, which corresponds to the limiting form of (3.2) for $\beta_B\gg1$.

Because of the simplifications introduced, the normalization condition given in (2.9) is satisfied only approximately by the steady radical profiles obtained from (5.8), exhibiting errors that are of order ε^2, i.e., $\int_0^\infty x^o d\xi\simeq1+(\pi\varepsilon)^2/6$. Consequently, $\Theta_N=0$ is no longer a solution to (5.10), being replaced in this simplified description by steady solutions with small positive values of Θ_N, of order ε^2, an outcome to be kept in mind. The linear stability analysis of the steady solutions to (5.10) then readily yields

$$b(1+\kappa)=\int_0^\infty\left(\frac{dx}{d\Theta_N}\right)_{\Theta_N=0}\exp(-\sigma(1+\kappa)\xi)d\xi, \tag{5.12}$$

a straightforward extension of (4.3), where use must be made of (5.8) and (5.11) to evaluate the derivative of $x(\xi,\Theta_N)$.

Equations (5.10) and (5.11) define the appropriate nonlinear evolution equation[2] for the chemistry considered here. Apart from the bifurcation parameter b and the acoustic parameter κ, only the two chemical-time ratios ε and ν of the corresponding steady detonation remain in the description. The limit of slow radical recombination serves, therefore, to link precisely the formulation of Clavin and He[2,3] to a realistic chemistry model, removing uncertainties associated with the model heat-release law utilized in their previous work.

Results of integrations of (5.10) with $\kappa=0$ for $\varepsilon=0.15$ and $\nu=3.46\times10^{-3}$ are exhibited in Fig. 7, while the corresponding results for $\varepsilon=0.05$ and $\nu=5.60\times10^{-9}$ are given in Fig. 8. Comparison between these results and those of Figs. 4 and 5 clearly indicates that (5.10) provides an accurate description of the detonation dynamics. Because of the approximations introduced in deriving (5.10), the values of b that characterize the transition between the different regimes differ slightly from those of the exact solution. Values of b associated with the neutrally stable solution of the first two modes, obtained in the present approximation from (5.12) with $\kappa=0$ in a manner analogous to the treatment of (3.1) but simpler in that the Runge–Kutta integrations are unnecessary, are given in Table II for comparison with the results in Table I. Typical differences are only a few percent.

The transition to long-period oscillations for $\varepsilon=0.05$ in Fig. 8 follows the sequence previously seen in Fig. 5. The two modes are present in the final solution when b falls in the range $0.65>b>0.61$. The plots corresponding to $b=0.63$ in Fig. 8 should be therefore compared with those corresponding to $b=0.61$ in Fig. 5. As can be seen, the validity of the simplified model that was derived in the limit $\bar{\varepsilon}\ll1$ extends far from the bifurcation point. Figures 7 and 8 indicate that, since the asymptotic description given in (5.8) produces exponentially small values of x everywhere as the crossover temperature is approached, (5.10) is even able to describe quenching events accurately.

TABLE II. The critical values of b (and the corresponding frequencies) of the neutrally stable solution of the modes with the two lowest frequencies as obtained from Eq. (5.12) with $\kappa=0$.

	$\varepsilon=0.05$	$\varepsilon=0.10$	$\varepsilon=0.15$
$\nu=5.60\times10^{-9}$:			
b_{C1} (ω_{C1})	0.678 (0.867)	1.078 (0.534)	1.408 (0.391)
b_{C2} (ω_{C2})	0.857 (6.438)	1.810 (3.153)	2.842 (2.053)
$\nu=1.23\times10^{-4}$:			
b_{C1} (ω_{C1})	0.384 (1.348)	0.681 (0.889)	0.946 (0.688)
b_{C2} (ω_{C2})	0.247 (13.20)	0.517 (6.432)	0.810 (4.175)
$\nu=3.46\times10^{-3}$:			
b_{C1} (ω_{C1})	0.253 (1.710)	0.461 (1.164)	0.644 (0.929)
b_{C2} (ω_{C2})	0.077 (20.35)	0.156 (9.913)	0.237 (6.435)

C. The parametric dependence of the stability boundary

For the values of the parameters selected above, two different oscillatory modes appeared associated with the dynamical behavior of overdriven detonations with chain-branching kinetics. Depending on the existing conditions, one or the other of the two modes was found to govern the initial oscillatory behavior as the solution bifurcates. Furthermore, the numerical results indicate that when the growth rates of the two modes are both positive, the one with a smaller frequency tends to dominate the final oscillatory solution. Since both modes may be relevant under different conditions, it is therefore of interest to characterize the stability domain of each of the two modes, expressing the results in terms of a limited number of chemical parameters.

Making use of (5.8) and of the expressions

$$\left(\frac{d\bar{\varepsilon}}{d\Theta_N}\right)_{\Theta_N=0}=-\varepsilon,\qquad \left(\frac{d\bar{\xi}_i}{d\Theta_N}\right)_{\Theta_N=0}=-\frac{\xi_i}{1-\varepsilon},\tag{5.13}$$

to evaluate the derivative $(dx/d\Theta_N)_{\Theta_N=0}$ allows us to write the quadrature appearing in (5.12) in the explicit form

$$\int_0^\infty\left(\frac{dx}{d\Theta_N}\right)_{\Theta_N=0}\exp(-\bar{\sigma}\xi)d\xi=-\frac{\xi_i}{1-\varepsilon}\int_{\xi_i}^\infty\frac{\exp(\xi_i-\xi)\exp(-\bar{\sigma}\xi)}{1+\exp[-(1-\varepsilon)(\xi-\xi_i)/\varepsilon]}d\xi$$
$$+\frac{1}{\varepsilon}\int_0^\infty\frac{\{1+H(\xi-\xi_i)[\exp(\xi_i-\xi)-1]\}\xi\exp(-\bar{\sigma}\xi)}{\exp[(1-\varepsilon)(\xi-\xi_i)/\varepsilon]\{1+\exp[-(1-\varepsilon)(\xi-\xi_i)/\varepsilon]\}^2}d\xi,\tag{5.14}$$

where the effect of acoustics has been taken into account in defining a modified complex number

$$\bar{\sigma}=(1+\kappa)\sigma.\tag{5.15}$$

To develop the needed simplified description, we employ the limit $\varepsilon\ll1$, for which the first quadrature on the right-hand side of the above equation reduces to

$$-\xi_i\exp(-\bar{\sigma}\xi_i)\int_{\xi_i}^\infty\exp[-(\xi-\xi_i)(\bar{\sigma}+1)]d\xi$$
$$=-\frac{\xi_i\exp(-\bar{\sigma}\xi_i)}{\bar{\sigma}+1},\tag{5.16}$$

if $\bar{\sigma}\varepsilon$ is small and gives a negligible contribution otherwise.

On the other hand, it can be seen that the denominator appearing in the second quadrature is exponentially large almost everywhere, remaining of order unity only for values of $\xi-\xi_i$ of order ε. Introducing the integration variable $s=-(1-\varepsilon)(\xi-\xi_i)/\varepsilon$ and neglecting small terms, of order ε or smaller, reduces this second quadrature to

$$\xi_i \exp(-\bar{\sigma}\xi_i)\int_{-\infty}^{\infty}\frac{\exp[-(\varepsilon\bar{\sigma}+1)s]}{(1+e^{-s})^2}ds = \xi_i\exp(-\bar{\sigma}\xi_i)\frac{\pi\varepsilon\bar{\sigma}}{\sin(\pi\varepsilon\bar{\sigma})}. \tag{5.17}$$

Adding now (5.16) and (5.17) and substituting the result into (5.12) yields, at the level of approximation utilized above

$$\bar{b}=\exp(-\bar{\sigma}\xi_i)\frac{\pi\varepsilon\bar{\sigma}}{\sin[\pi\varepsilon(\bar{\sigma}+1)]}, \tag{5.18}$$

as an implicit equation for $\bar{\sigma}$ in terms of the parameters ξ_i, ε and

$$\bar{b}=\frac{b(1+\kappa)}{\xi_i}=\frac{1+\kappa}{(\gamma-1)\beta_B q\xi_i} \simeq \frac{1+\sqrt{(\gamma+1)(q+1)/(8\gamma q d)}}{(\gamma-1)\beta_B q\varepsilon\ln(\nu^{-1})}. \tag{5.19}$$

This last expression defines a modified bifurcation parameter for describing the stability boundary. Since terms of the form $\varepsilon\bar{\sigma}$ are retained in the derivation of (5.18), the resultant equation adequately describes in particular the high-frequency behavior corresponding to large values of ω, of order ε^{-1}. Equation (5.18) reveals that the stability of the steady solution depends on the two chemical time ratios ε and ξ_i, with the effect of acoustics entering as a small correction to the resulting oscillation frequency. To determine the stability domain of each of the two relevant modes, we investigate neutrally stable solutions $\bar{\sigma}=\bar{\omega}i=(1+\kappa)\omega i$. Appropriate simplified expressions for the values of $\bar{\omega}$ and $\bar{b}$ corresponding to the two modes can be obtained from (5.18) by considering separately the cases $\bar{\omega}\sim O(1)$ and $\bar{\omega}\gg 1$.

With $\bar{\omega}\sim O(1)$, taking the asymptotic limit $\varepsilon\ll 1$ results in the approximate expression

$$\bar{b}=\exp(-i\bar{\omega}\xi_i)\bar{\omega}(\bar{\omega}+i)/(1+\bar{\omega}^2). \tag{5.20}$$

Solving the imaginary and real parts of this equation separately gives the critical value of the bifurcation parameter

$$\bar{b}_{C_1}=\cos(\bar{\omega}_{C_1}\xi_i), \tag{5.21}$$

where the frequency of the neutrally stable solution is determined from the implicit equation

$$\bar{\omega}_{C_1}\tan(\bar{\omega}_{C_1}\xi_i)=1. \tag{5.22}$$

The results depend only on the nondimensional induction length and are shown in Fig. 9. From (5.22), it can be easily shown that $\bar{\omega}_{C_1}\xi_i$ reaches its maximum value $\bar{\omega}_{C_1}\xi_i=\pi/2$ as $\xi_i\gg 1$. Using this last result yields $2\pi/(\omega_{C_1}\xi_i)=4(1+\kappa)$ for

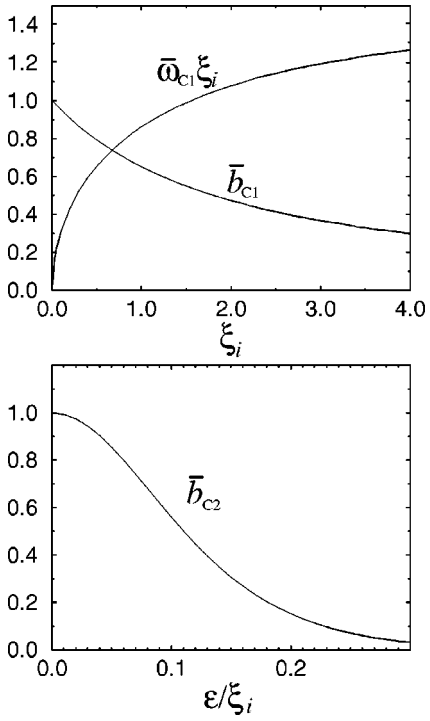

FIG. 9. The values of $\bar{b}_{C1}$, $\bar{\omega}_{C1}\xi_i$, and $\bar{b}_{C2}$ as obtained from (5.21), (5.22), and (5.26).

the minimum value of P/ξ_i, revealing that the period of the resulting oscillation, although of the order of the induction time t_i, is always larger by a significant amount.

The limiting form of (5.18) for $\bar{\omega}\gg 1$ can be written in the first approximation as

$$\ln(\bar{b})=i(2\pi n-\bar{\omega}\xi_i)+\ln\left(\frac{2\pi\varepsilon\bar{\omega}}{\exp(\pi\varepsilon\bar{\omega})-\exp(-\pi\varepsilon\bar{\omega})}\right), \tag{5.23}$$

an equation that can be solved to give

$$\bar{\omega}\xi_i=2\pi n,\quad \bar{b}=\frac{2\pi\varepsilon\bar{\omega}}{\exp(\pi\varepsilon\bar{\omega})-\exp(-\pi\varepsilon\bar{\omega})}, \tag{5.24}$$

where $n=1,2,\ldots$. Apart from the small acoustic correction, the associated periods become integer fractions of the induction time according to $P/\xi_i=(1+\kappa)/n$. The most unstable mode, that is, the one with the largest associated value of $\bar{b}$, corresponds to

$$\bar{\omega}_{C_2}\xi_i=2\pi, \tag{5.25}$$

yielding

$$\bar{b}_{C_2}=\frac{4\pi^2\varepsilon/\xi_i}{\exp(2\pi^2\varepsilon/\xi_i)-\exp(-2\pi^2\varepsilon/\xi_i)}, \tag{5.26}$$

as the critical value of the bifurcation parameter. Equation (5.25) states that the period of this second mode is equal to the induction time of the steady detonation plus an additional acoustic delay, that is, $P/\xi_i=1+\kappa$. The dependence of $\bar{b}_{C_2}$ on the ratio of the branching time to the induction time,

ε/ξ_i, is also exhibited in Fig. 9. This solution may be expected to become inaccurate at large values of ξ_i.

The agreement between the predictions given in (5.21), (5.22), (5.25), and (5.26) and those obtained by integrating numerically (4.3) is satisfactory, with discrepancies being of order ε. The results provide, therefore, a simple quantitative description for the frequencies and stability boundaries of the two relevant modes of instability. The results indicate that the stability boundary can be better described in terms of the modified bifurcation parameter defined in (5.19), with overdriven detonations with $\bar{b}>1$ being always stable to planar disturbances. Since the model chemistry employed contains the most relevant features of general chain-branching kinetics, it is expected that a similar stability condition holds in realistic systems.

VI. CONCLUSIONS

Branched-chain detonations for which the heat release is dominated by recombination possess a bifurcation parameter $\bar{b}$ defined in (5.19). At large values of this parameter, the detonations are stable to pulsations, but they become unstable when this parameter is small. The time-dependent one-dimensional dynamical behavior depends mainly on three parameters, $\bar{b}$, the ratio ξ_i of the induction time t_i to the recombination time A_R^{-1} and the ratio ε of the e-folding branching time $W/[A_B\rho_N^o Y_F \exp(-\beta_B)]$ to A_R^{-1}. For most real detonations of practical interest, ε is small and ξ_i is roughly of order unity. The ''crossover'' condition considered previously,[15] at which the rate of the branching step is of the same order as the rate of the recombination step, corresponds to ε being of order unity, and steady detonations cannot exist when ε exceeds unity, because recombination rates are then too large compared with branching rates for the chemistry to proceed. The present study is focused on small values of ε, not thoroughly explored previously, where branching is rapid compared with recombination, and the dependence on the new bifurcation parameter $\bar{b}$ is investigated for fixed values of ε. It is found that if $\bar{b}$ is decreased below a critical value of order unity, roughly independent of the values of ξ_i and ε, then a pulsating instability sets in, the amplitude of which increases with decreasing $\bar{b}$, soon leading to failure of the detonation when $\bar{b}$ is decreased below another critical value.

Two different types of modes of pulsation are found to exist near bifurcation for small ε. One is a low-frequency mode in which the oscillation period is somewhat larger than the transit time through the induction region, although typically of the same order. The other is a set of high-frequency modes whose periods are integer fractions of this same transit time. All of the modes, including the low-frequency mode, are rapid compared with the slow mode derived in earlier work by applying ideas of activation-energy asymptotics to one-step Arrhenius models. As the ratio ξ_i of induction to recombination time increases, however, the period of the low-frequency mode lengthens and at least in a qualitative sense approaches the simplified one-step Arrhenius prediction, as might be expected since in this limit heat release becomes short compared with induction, and induction is strongly temperature sensitive. The period also is lengthened somewhat by acoustics because of the associated nonzero time required for a signal to return upstream to the shock.

The mode encountered first as $\bar{b}$ decreases and bifurcation begins depends on the value of ε. Since the conditions explored are restricted mainly to ξ_i of order unity, decreasing ε may be viewed as decreasing the ratio of the branching to recombination time or as decreasing the ratio ε/ξ_i of branching to induction time. For values of this branching to recombination or induction time ratio larger than about 0.1, the low-frequency mode bifurcates first and dominates the dynamics for all values of $\bar{b}$. For smaller values than this, however, values which are of physical relevance in many chemical systems, it is a high-frequency mode that first bifurcates, and the dynamics in the vicinity of the bifurcation is dominated by the high-frequency mode. As $\bar{b}$ is decreased further and the nonlinearity of the oscillations increases, the low-frequency mode bifurcates and begins to dominate the dynamics, being affected by the high-frequency mode only at early times. There is a narrow intermediate range of values of $\bar{b}$ in which influences of both modes clearly persist for all time. At small values of $\bar{b}$ where detonation failure is approached, the low-frequency mode becomes highly dominant and highly nonlinear. It was not possible numerically to ascertain whether period doubling or chaos set in prior to failure. If this does occur, then it does so over a very small range of $\bar{b}$. It is possible that these phenomena do not exist at the small values of ε addressed here; they were identified previously[15] only for relatively large values of ε. If ε were to be decreased further, below the lowest value, 0.05, for which calculations were performed here, the extent of domination by high-frequency phenomena would increase, and importance of additional high-frequency modes possibly could emerge. This range of very small ε and ε/ξ_i is of physical interest and deserves investigation in the future.

The physical meaning of the bifurcation parameter $\bar{b}$ in (5.19) needs discussion here, beyond that given previously[2–4] for the related generic parameter b which does not pertain specifically to branched-chain kinetics. A number of different influences occur in $\bar{b}$. One is the factor $(\gamma-1)$; the more the specific-heat ratio differs from unity, the greater is the tendency towards instability. The present theory incorporates acoustic effects as a perturbation to the dynamics of overdriven detonations. As previously explained,[3] decreasing values of the overdrive parameter d (increasing values of κ) promote stability, that is, acoustics are stabilizing. Increasing β_B, the branching activation energy referred to the thermal enthalpy at the Neumann state, increases the tendency towards instability, as does increasing q, the heat release referred to this same enthalpy. The product of $(\gamma-1)$ with these two quantities, $(1+\kappa)^{-1}$ and the ratio ξ_i of induction time to recombination time is the parameter $\bar{b}^{-1}$ that mainly controls the stability behavior for branched-chain chemistry. Thus, for example, increasing the induction time promotes instability, while increasing the recombination time tends to suppress it. The effects of acous-

tics, heat release, temperature sensitivity of branching, induction period and recombination rate thus all are folded into this single bifurcation parameter. Especially for short branching times, which is the situation generally encountered in detonations with branched-chain chemistry, all of these phenomena play roles in the one-dimensional stability and dynamics, striking a delicate balance in which the variation of any one of them, with the others held fixed, affects the detonation behavior. It is satisfying to have identified just one parameter that captures all of these effects.

ACKNOWLEDGMENTS

The work of A.L.S. and M.C. was supported by the Spanish CICYT under Contracts Nos. PB95-0296 and PB98-0142-C04, while the work of P.C. was supported by the Institut Universitaire de France and that of F.A.W. by the National Science Foundation through Grant No. CTS 9812996. During the development of this work M.C. was on a leave of absence from the Spanish MEC.

[1]W. Fickett, J. D. Jacobson, and G. L. Schott, ''Calculated pulsating one-dimensional detonations with induction-zone kinetics,'' AIAA J. **10**, 514 (1972).
[2]P. Clavin and L. He, ''Stability and nonlinear dynamics of one-dimensional overdriven detonations in gases,'' J. Fluid Mech. **306**, 353 (1996).
[3]P. Clavin and L. He, ''Acoustic effects in the nonlinear oscillations of planar detonations,'' Phys. Rev. E **53**, 4778 (1996).
[4]P. Clavin, L. He, and F. A. Williams, ''Multidimensional stability analysis of overdriven gaseous detonations,'' Phys. Fluids **9**, 3764 (1997).
[5]Y. B. Zeldovich, ''On the theory of flame propagation,'' Zh. Fiz. Khim. **22**, 27 (1948), English translation (1951), Tech. Memo. 1282, National Advisory Committee of Aeronautics, Washington, DC.
[6]Y. B. Zeldovich, ''Chain reactions in hot flames: An approximate theory of flame velocities,'' Kinet. Katal. **11**, 305 (1961).
[7]B. F. Gray and C. H. Yang, ''On the unification of the thermal and chain theories of explosion limits,'' J. Phys. Chem. **69**, 2747 (1965).
[8]A. Liñán, ''A theoretical analysis of premixed flame propagation with an isothermal chain reaction,'' Instituto Nacional de Técnica Aeroespacial ''Esteban Terradas'' (Madrid), USAFOSR Contract No. E00AR68-0031, Technical Report No. 1, 1971.
[9]A. K. Kapila, ''Homogeneous branched-chain explosion: Initiation to completion,'' J. Eng. Math. **12**, 221 (1978).
[10]N. N. Semenov, *Chemical Kinetics and Chain Reactions* (Oxford University Press, New York, 1935).
[11]R. A. Strehlow, *Fundamentals of Combustion* (International Textbook, Scranton, PA, 1968), p. 108.
[12]Y. B. Zeldovich, G. I. Barenblatt, V. B. Librovich, and G. M. Makhviladze, *The Mathematical Theory of Combustion and Explosions* (Consultants Bureau, New York, 1985), pp. 393–401.
[13]F. A. Williams, *Combustion Theory*, 2nd ed. (Addison Wesley, Redwood City, CA, 1985), p. 570.
[14]M. Short and J. W. Dold, ''Linear stability of a detonation wave with a model three-step branching reaction,'' Math. Comput. Modelling **24**, 115 (1996).
[15]M. Short and J. J. Quirk, ''On the nonlinear stability and detonability limit of a detonation wave for a model three-step chain-branching reaction,'' J. Fluid Mech. **339**, 89 (1997).
[16]P. A. Blythe and D. G. Crighton, ''Shock-generated ignition: The induction zone,'' Proc. R. Soc. London, Ser. A **426**, 189 (1989).
[17]G. Balakrishnan and F. A. Williams, ''Turbulent combustion regimes for hypersonic propulsion employing hydrogen-air diffusion flames,'' J. Propul. Power **10**, 434 (1994).
[18]K. A. Bhaskaran, M. C. Gupta, and T. H. Just, ''Shock tube study of the effect of unsymmetric dimethyl hydrazine on the ignition characteristics of hydrogen mixtures,'' Combust. Flame **21**, 45 (1973).
[19]B. Lewis and G. Von Elbe, *Combustion, Flames and Explosions of Gases* (Pergamon, New York, 1951).
[20]A. L. Sánchez, A. Liñán, and F. A. Williams, ''A WKB analysis of radical growth in the hydrogen-air mixing layer,'' J. Eng. Math. **31**, 119 (1997).
[21]A. L. Sánchez, I. Iglesias, and A. Liñán, ''An asymptotic analysis of chain-branching ignition in the laminar wake of a splitter plate separating streams of hydrogen and oxygen,'' Combust. Theory Modell. **2**, 259 (1998).
[22]A. L. Sánchez, A. Liñán, and F. A. Williams, '''Chain-branching explosions in mixing layers,'' SIAM (Soc. Ind. Appl. Math.) J. Appl. Math. **59**, 1335 (1999).
[23]L. L. Bonilla, A. L. Sánchez, and M. Carretero, ''The description of homogeneous branched-chain explosions with slow radical recombination by self-adjusting time scales,'' SIAM (Soc. Ind. Appl. Math.) J. Appl. Math. **61**, 528 (2000).